

RESEARCH PAPER

Growth of wurtzite ZnO nanorods using different capping agents: Characterization, morphology, and investigation the catalytic activity in some oxindoles and indolyl organics

Maryam Haghighi *, Kobra Nikoofar *, Zeinab Ahmadvand

Department of Chemistry, Faculty of Physics and Chemistry, Alzahra University, Tehran, Iran

ARTICLE INFO

Article History:

Received 22 March 2018

Accepted 26 June 2018

Published 1 August 2018

Keywords:

3,3-Di(indolyl)indoline-2-ones

Capping Agent

Tris(indolyl)methane

ZnO NR

ABSTRACT

ZnO nanorods have been prepared through chemical deposition of $\text{Zn}(\text{OAc})_2 \cdot 2\text{H}_2\text{O}$ by employing different capping agents, (PEG, MW=2000 and PEG, MW=5000). The fabricated catalyst was characterized by scanning electron microscope (SEM) images and XRD pattern. The results show the one dimensional growth of ZnO nano-rods. The capping agents can control the shape and growth of nano-sized crystals. The vertically aligned ZnO was fabricated by PEG 2000, but PEG 5000 changes the ZnO nano-rods to elbow shape. The synthesized nano-rodes have been utilized as highly efficient catalyst to promote some one-pot multicomponent reactions (MCRs) of indoles consist of symmetrical and unsymmetrical 3,3-di(indolyl) indoline-2-ones and tris(indolyl)methanes synthesis under mild reaction conditions, respectively. Comparison of the catalytic power of these two kinds of synthetic ZnO NRs (2000 & 5000) has also been investigated. Importantly, the catalysts can be recovered from the reaction media and reused for four runs without any activity loss.

How to cite this article

Haghighi M, Nikoofar K, Ahmadvand Z. Growth of wurtzite ZnO nanorods using different capping agents: Characterization, morphology, and investigation the catalytic activity in some oxindoles and indolyl organics. *Nanochem Res*, 2018; 3(2):131-141. DOI: 10.22036/ncr.2018.02.002

INTRODUCTION

Nano-size materials with high surface area ratio can alter chemical and physical properties and have been considered more in recent decade [1,2]. Metal nano-oxides have been gained attention in recent years due to their new exciting industrial applications as photocatalysts, semiconductors, gas sensors, thermal conductive nano-particles and solar energy convertors [3-8]. They have been developed as proper candidate as catalyst due their unique properties [9-12]. It has been shown that material properties such as energy bond gap and thermal conductivity are size dependent [13,14]. Among the various nano-materials, zinc oxides (ZnO) have been applied as photocatalysts, antibacterial materials, and optoelectronic devices

[15-17]. Currently, the optoelectronic application of ZnO nano-sized particles were widespread owing to high exciting energy (60 meV) and wide energy band gap (3.37 eV) [18]. Up to now, various ZnO nano-structures with different morphologies have been synthesized such as nano-particles [19], nano-tubes [20], nano-wires [21], nano-flowers [22], nano-belts [23] and nano-rods [24].

Some synthesis methods are based on the use of toxic capping gents and solvents. Therefore many efforts have been devoted to substitute green approaches using non-toxic materials. Tragacanth as a biotemplate was carried out for metal oxide nanoparticle synthesis and ferrite nanocomposites [25-27]. However, the sol-gel using tragacanth is a simple and cost effective method for preparation of nanomagnetic $\text{NiFe}_2\text{O}_4/\text{ZnO}$ [28]. As an

* Corresponding Author Email: m.haghighi@alzahra.ac.ir
k.nikoofar@alzahra.ac.ir

alternative, the oak fruit hull and Arabic gum have been introduced as convenient and low cost biomaterials for synthesis of the bimetallic nano oxides and nickel oxide [29-31]. In continuation Arabic gum was proposed for magnesium oxide and zinc oxide nanoparticles over sol-gel method [32, 33]. It was found that magnesium ferrite with attractive catalytic properties such as degradation of dyes; can be prepared using sol-gel method over tragacanth gum [34, 25]. In addition ferulago angulate and black tea extract were proposed as convenient biomaterial for ZnO nano particles [35, 36].

In the past few years, diverse preparation methods have been proposed for the synthesis of ZnO nano-crystals. Moreover, various physical, electrochemical and chemical deposition methods have been developed for the synthesis of 1D vertically aligned ZnO NRs. The sol-gel precipitation method in alcoholic solution is commonly used for simple obtaining of ZnO NRs [37]. In addition, hydrothermal method [38], sputtering [39], electrochemical reaction [40], and molecular beam epitaxy [41] have been reported and applied in different studies. Most of these techniques are expensive and difficult, especially to control the size and crystal uniformity [1]. Pulsed laser ablation is one of the precise methods for ZnO nano-sized obtained in recent years [42, 43]. Although this technique is a controlled fabrication method, but it is more expensive. Chemical deposition method is an important, applied and efficient technique. Different synthesis routes have been proposed with different capping agents and by adjusting various parameters such as pH value, temperature and reflux time.

Multi-component reactions (MCRs) have attracted for organic chemists recently because of their highlighted advantages such as atom economy, convergence, high productivity, ease of implementation, excellent products yields, and large-range of application in organic and medicinal chemistry. N-containing heterocyclic MCRs have gained in great interest because of the importance of nitrogen in drugs as well of natural products branches [44-46].

In this research, a chemical precipitation method was used and modified for ZnO NR fabrication. The self-assembly nano-rods were obtained in the presence of PEG 2000 & 5000. The one dimensional structure of ZnO NR was characterized and studied for two aforementioned surfactants. In the other word, the effect of different capping agents on

the shape and size of nano-rods were studied and compared. The experiments show different chemical routes affect crystalline size and structure. It was found that catalytic activity of some organic transformations can be improved by using ZnO NRs.

EXPERIMENTAL

Materials and methods

Zinc acetate dehydrate $\text{Zn}(\text{OA})_2 \cdot 2\text{H}_2\text{O}$, PEG 2000, PEG 5000, and all other chemicals and solvents were purchased from Merck company. In the present work, deionized water and NH_3 (Merck, 25%) were used. Nano-crystal characteristics were observed and performed by X-ray diffractometer (Philips, with $\text{CuK}\alpha 1$ radiation, cobalt anode with wave length 1.7889, 40 kV, 40 mA), and scanning electron microscope (SEM, model EM 3200, kyky). $^1\text{H-NMR}$ spectra were recorded in CDCl_3 solvent on a Bruker 400 MHz spectrometer. Melting points were determined using a Stuart Scientific SMP2 capillary apparatus and are uncorrected.

Procedure for the synthesis of ZnO NRs

A typical and simple chemical deposition method was employed for the synthesis of ZnO NRs [47]. Briefly, $\text{Zn}(\text{OA})_2 \cdot 2\text{H}_2\text{O}$ (1g) and PEG 2000 (0.3g) were dissolved in 140 mL double distilled water to obtain a clear and transparent solution. 1.5 mL NH_3 (25%) was added drop wise to form an alkaline solution. The solution was stirred and refluxed for 6 h at 80. It was cooled, centrifuged and washed with distilled water and ethanol for more times. The precipitant was stirred with 90 mL double distilled water and refluxed for 9 h to complete the reaction. The solution was cooled again, centrifuged and washed with absolute ethanol. Then, the participant was dried in an oven at 100. The ZnO NRs have been prepared and studied in the next section. Surface clean nano-rods were obtained by capping agent removal.

General procedure for preparation of symmetrical and unsymmetrical 3,3-di(indolyl)indoline-2-ones

A mixture of indoles **1a-e** or pyrrole (2 mmol), isatins **2a-d** (1 mmol), H_2O (5 mL), and ZnO NRs (15 mol%) were added to a 25 mL flask equipped with a condenser and refluxed by constant stirring for appropriate time as shown in Table 3. The progress of the reactions monitored by thin layer chromatography (TLC) technique. After reaction completion, the mixture was diluted with EtOAc (10 mL) and centrifuged to remove the catalyst.

The filtrate was extracted with water and further EtOAc (2×10 mL), the organic layer dried over anhydrous MgSO₄ and evaporated under reduced pressure. The resulting crude residue was purified by column chromatography on silica gel to afford the pure symmetrical products **3a-k**. In the case of unsymmetrical 3,3-di(indolyl)indoline-2-ones, in the first step of the domino-MCR, appropriate indoles **1a-d** (1mmol), isatins **2a-b** (1 mmol), H₂O (5 mL), and ZnO NRs (15 mol%) were refluxed in a vessel equipped with condenser to provide the 3-hydroxy-3-(indolyl)indolin-2-ones as intermediate compounds. The reaction conversion was checked by TLC. Then 1 mmol of an appropriate indole was added to the flask and refluxed to perform their corresponding unsymmetrical 3,3-di(indolyl)indoline-2-ones **3l-r**. The work-up procedure is the same as symmetrical analogs. All the products were known and characterized by comparison of their melting points and ¹H-NMR data with those of the authentic samples in literature.

General procedure for tris(indolyl)methanes synthesis

A mixture of indoles **1a-d** (3 mmol), triethylorthoformate **4** (3 mmol), and ZnO NRs (15 mol%) heated by vigorous magnetic stirring at 110 for the appropriate time needed for completion that was monitored by TLC method (Table 4). The solid residue diluted with EtOAc (10 mL) and centrifuged to remove ZnO. Extraction the filtrate with EtOAc, drying over anhydrous MgSO₄ and evaporation the solvent followed by purification through column chromatography on silica-gel lead to the correspondence tris(indolyl)methanes **5a-d**.

Recycling of ZnO NRs

Upon the completion of compounds **3a** and **6a**, the ZnO NRs that were separated via centrifuging, washed with EtOAc (2×10 mL), dried and reused for the similar reactions. The recovery and catalyst usage was repeated within four runs without noteworthy loss of catalytic activity.

RESULTS AND DISCUSSION

Morphology of ZnO NRs

In this section, the structure and morphology of ZnO nano-rods were obtained and considered. The XRD pattern of obtained nano-rods is shown in Fig. 1 that angles were reported for cobalt anode with wave length 1.7889 Å. The 2θ values were multiplied in 0.86 for Cu anode. The peaks values in the presence of PEG 2000, were observed at the following scattering angles (2θ) 31.8, 34.5, 36.4, 47.9, 57.3, 64.1, 67.8, 69.5 and 70.8. These peaks correspond to the reflection from 100, 002, 101, 102, 110, 103, 200, 112 and 201 crystal planes, respectively and identified the hexagonal Wurtzite unit cell (according to JCPDS No. 36-1451 for ZnO). XRD figures show non central symmetry and polar surfaces [48-50]. Furthermore, no significant shifts of peaks are recorded, which indicates that there are any impurities such as capping agents or other solvents and other ZnO nano-structures.

Figs. 2 and 3 show the XRD pattern for products (by PEG 2000 & PEG 5000). X-ray diffraction plot of ZnO NRs fabricated using PEG 5000, is shown in Fig. 3. The peaks for this case were observed at the angles (2θ) 31.8, 34.5, 36.4, 48.03, 57.5, 64, 67.9, 69.5 and 70.8. In the other hand, the peaks correspond to Wurtzite nano-crystal planes precisely for both cases.

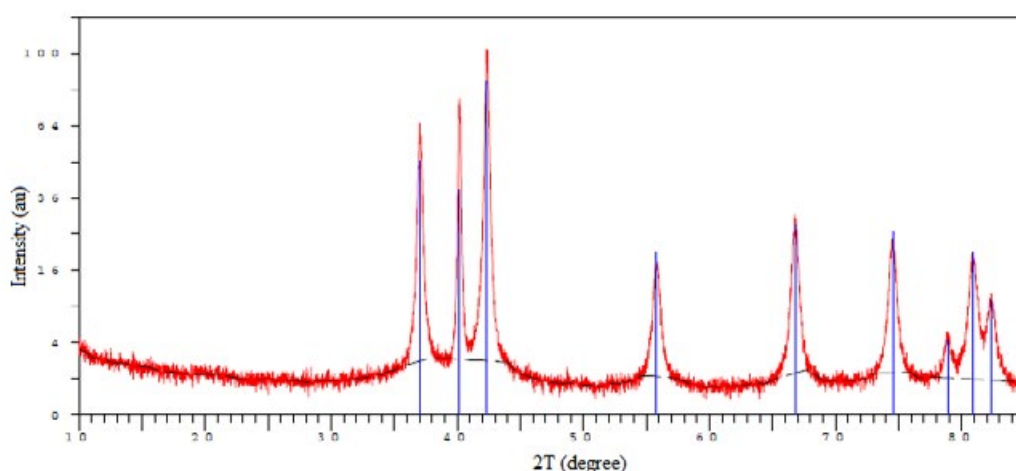


Fig. 1. XRD of ZnO NRs were obtained by PEG 2000 (The angles are reported for Cobalt anode $\lambda=1.78\text{\AA}$).

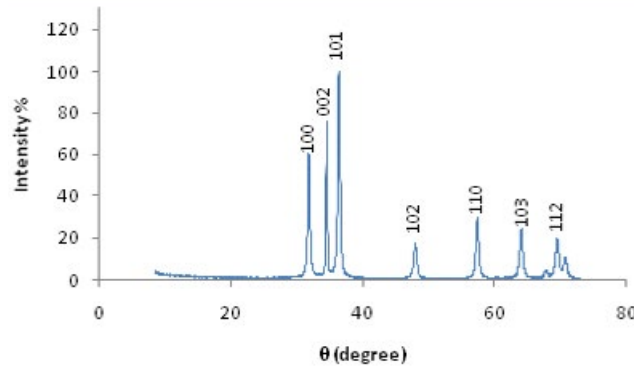


Fig. 2. XRD pattern of ZnO nano-crystal fabricated by PEG 2000 (The angles are reported for Cu anode $\lambda=1.54\text{\AA}$).

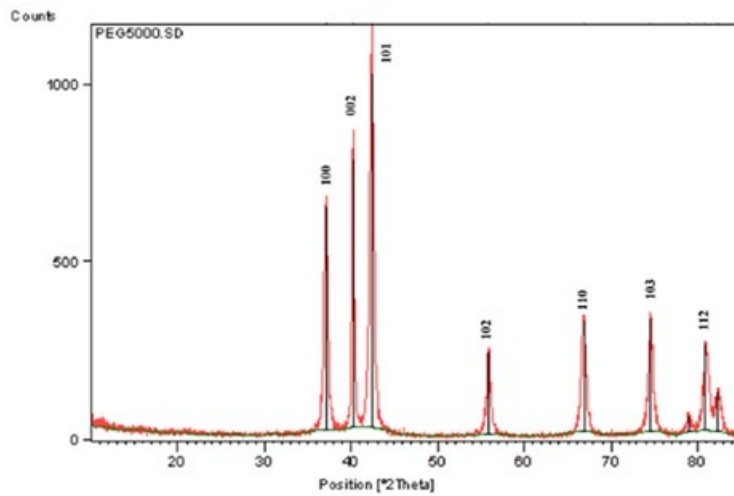


Fig. 3. XRD pattern of ZnO nano-crystal fabricated by PEG 5000 (The angles are reported for Cobalt anode $\lambda=1.78\text{\AA}$).

In continue, the average diameter of ZnO NRs has been estimated using Scherrer formula [51]:

$$d = k\lambda/\beta \cos \theta \quad (1)$$

Where λ is wavelength of the X-ray ($\lambda=1.54\text{\AA}$ for Cu anode & $\lambda=1.78\text{\AA}$ for Co anode), β =FWHM (full width at half maximum in radians) of the diffraction peak, θ is the Bragg's diffraction angle, and k is a constant between 0.89 and 1. This formula represents a simple relationship between crystal size and peak broadening. Peak broadening is due to the size of nano-crystal, strain and instrumental broadening. Then, β is defined by following formula:

$$\beta = \beta_{size} + \beta_{ins} + \beta_{strain} \quad (2)$$

β_{strain} expresses micro strain that have been

observed by stocks and Wilson in 1944 [52]. This term emerges due to imperfect crystals. Also, an accurate equation must be account instrumental broadening effect (β_{ins}). In this work, strain malfunction on XRD pattern was neglected but β_{ins} was accounted by XRD pattern of instrument. This allows us to accurate calculation of nano-rods diameter. Particle size of ZnO nano-rods were calculated in the presence of PEG 2000 and PEG 5000. The estimated crystallite size using Scherrer's formula is of the same order s in SEM images. Mean particle diameter was calculated 21 nm in the presence of PEG 2000 as capping agent and 36 nm for PEG 5000. For this case, β_{ins} was estimated 0.0033 radians based on instrumental XRD pattern.

Capping agents are frequently used in nanoparticle synthesis to prevent overgrowth and aggregation as well as to control the size of nanoparticle in a precise way. Capping agents

could be stopped the nanoparticles and nano-rods growth. Stabilizing agents were added to the initial solution to prevent agglomeration of the nano-rods. The above mentioned materials play different roles which result various products. Here too, dispersing agent helps to prevent agglomeration, but the final product must be a liquid or suspension [53].

PEG could serve all of the three aforementioned roles that were commonly used by different researchers. In this work, the effects of two different capping agents (PEG 2000 & PEG 5000) on ZnO NRs growth were studied and analyzed. The residual capping agents have adverse and favorable behaviors in catalytic applications of ZnO NRs. The capping agents usually act as a physical barrier to restrict the free access of reactant to catalytic nano-powders; they can also be utilized to promote heterogeneous catalytic performance of nano-crystals. Due to the complexity of these opposite effects, a general and complete survey of capping agents in nano-catalysis is therefore necessary. The adverse impact on heterogeneous catalytic reactions has been not studied precisely which is therefore necessary. The characteristics, shape, size, growth manner and catalytic performance of ZnO NRs were studied in this research. The SEM images

of ZnO nano-rods are cylindrical in morphology that were shown in Fig. 4. S_5 is ZnO NRs which were prepared by PEG 2000. SEM images confirm vertically aligned growth of ZnO nano-rods. The diameter of S_5 (by PEG 2000) nano rods is in the range of 35-50 nm that can be seen in Fig. 4(a). It is apparent from SEM images that diverse shapes of nano-crystals were obtained using PEG 5000. The SEM micrograph of S_6 (by PEG 5000) shows an elbow in the presence of PEG 5000. Both S_5 and S_6 have homogeneous morphology.

PEG 5000 changes the growth habit of ZnO nano-rods and can control the shape of their lattices. Although XRD pattern shows Wurtzite nano-structure, the fabricated ZnO was bow and have not been vertically aligned. Interestingly, this shape is being reported for the first time whereas for different capping agent. In the other word, PEG can control the crystal shape by changing the orientation of rods.

Investigation the catalytic activity of synthesized ZnO NRs

The catalytic activities of synthesized ZnO NRs (Fabricated by PEG 2000 & PEG 5000) have been evaluated in some MCRs on the basis of

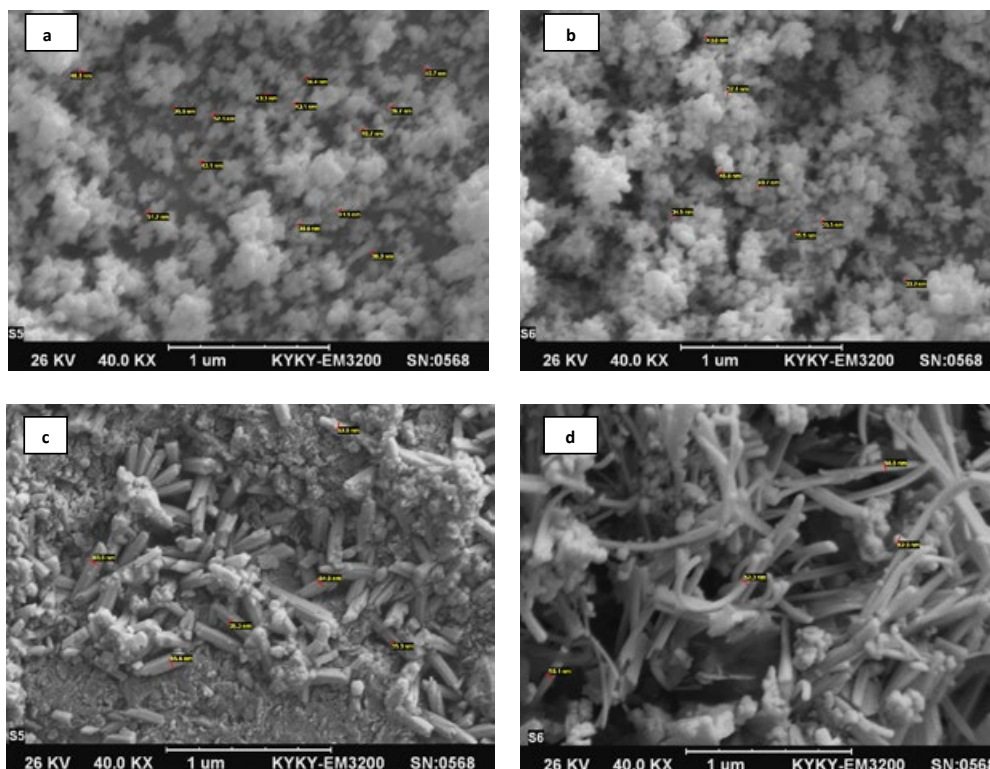


Fig. 4. The SEM images of ZnO NRs 2000 (a, b) & ZnO NRs 5000 (c, d).

indole ring. Indole moiety is featured in variety of pharmacologically and biologically active compounds [54]. Among a wide-range of substituted indole-based heterocycles, 3,3-di(indolyl)indoline-2-ones and tris(indolyl)methanes (TIMs) possess special position. The former contains anticancer [55], antimicrobial [56], and antiinflammatory [57]. TIMs serves bacterial metabolites and cytotoxic agents [58].

Due to strategic situation of these classes in organic and biological chemistry, herein we focus on their synthesis utilizing newly synthesized ZnO NRs. In the first step, some reactions have been schematized using model substrates to optimize the reaction conditions using ZnO 2000 nanoparticles

as catalyst. Results are summarized in Table 1 for 3,3-di(indolyl)indoline-2-ones, and Table 2 for TIMs. As expected in Table 1 the typical production of compound **3a**, obtained in H₂O as solvent under reflux conditions are at the highest yield (entry 3). Performing the model reaction at ambient temperature 70 (entry 2) and room temperature (entry 4) caused moderate yields. Comparing the data of entry 3 and 5 confirms that decreasing the ZnO mole ratio leads to increasing the reaction time. Also, the experiments show that increasing temperature and catalyst mole ratio don't affect the reaction progress considerably.

Perceiving data of Table 2, the model reaction of TIM synthesis was the condensation of indole

Table 1. Screening the optimized reaction condition for the synthesis of **3a**.

Entry	Conditions (1a/2a mole ratio/ ZnO NR amount/ solvent/ temperature)	Time (h)	Yield (%)
1	2:1/ 15 mol%/ solvent-free/ 110 °C	1	70
2	2:1/ 15 mol%/ H ₂ O/ 70 °C	1	70
3	2:1/ 15 mol%/ H ₂ O/ reflux	1	88
4	2:1/ 15 mol%/ H ₂ O/ r.t.	1	55
5	2:1/ 10 mol%/ H ₂ O/ reflux	1.5	85

Table 2. Optimizing the reaction conditions for **5a** preparation.

Entry	Conditions (1a/4 mole ratio/ZnO NR amount/ solvent/ temperature)	Time (h)	Yield (%)
1	3:3/ 15 mol%/ solvent-free/ 110°C	1	98
2	3:3/ 15 mol%/ H ₂ O/ reflux	5	<20
3	3:3/ 15 mol%/ MeOH/ reflux	2.5	88
4	3:3/ 15 mol%/ solvent-free/ 90°C	1	78
5	3:3/ 15 mol%/ solvent-free/ rt	5	38
6	3:2/ 15 mol%/ solvent-free/ 110°C	1	85
7	3:3/ 10 mol%/ solvent-free/ 110 °C	1	68

with triethylorthoformate that accomplished under solvent-free conditions at 110 (entry 1). Diminution the temperature to 90, declines the reaction yield (entry 4). Decreasing the amount of **4** (entry 6) or ZnO NRs mole ratio (entry 7), discounted the reaction yield.

After denotation the optimized conditions for the synthesis of these two classes of compounds, in the second step, different derivatives of 3,3-di(indolyl)indoline-2-ones have been prepared (Table 3). Attending the whole results in Table 3, demonstrated the ZnO NRs (2000) efficacy in the

synthesis of symmetrical 3,3-di(indolyl)indoline-2-ones via the condensation reaction of various electron-deficient and electron-rich indoles and isatins (entries 1-9). Condensation of 3-methylindole with isatin at its 2-position, is another noteworthy potential of the catalyst (entry 10). To illustrate the widespread applicability of the catalyst, condensation of pyrrole and isatin occurred on its C-2 position to create product **3k** (entry 11). Moreover ZnO NRs (2000) catalyzed preparation variety of unsymmetrical 3,3-di(indolyl)indoline-2-ones prosperously (entry 12-18).

Table 3. Investigation of ZnO NRs catalytic activity in 3,3-di(indolyl)indolin-2-ones synthesis.

1a: R₁=R₂=R₃=H

1b: R₁=R₃=H, R₂=CH₃

1c: R₁=CH₃, R₂=R₃=H

1d: R₁=R₂=H, R₃=Br

2a: R₄=R₅=H

2b: R₄=CH₂C₆H₅, R₅=H

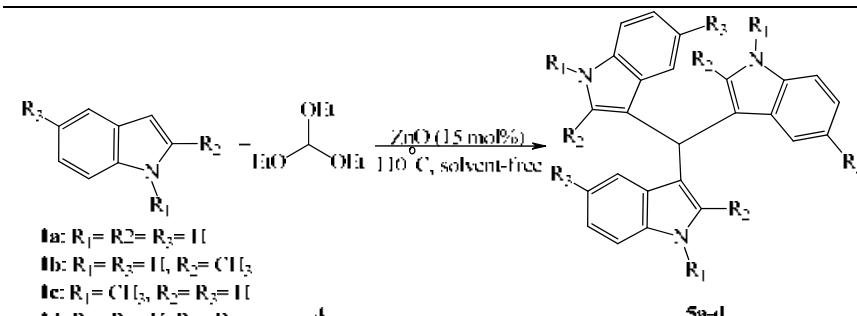
2c: R₄=CH₃, R₅=H

2d: R₄=H, R₅=Br

3a-r

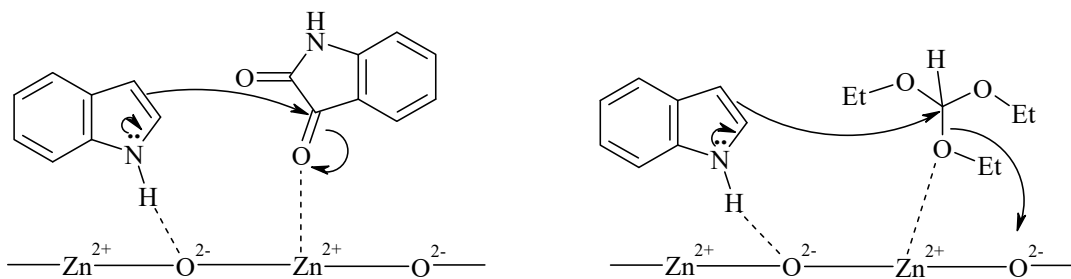
Entry	Indole	Isatin	Product	ZnO NRs (2000)		ZnO NRs (5000)	
				Time (h)	Yield (%)	Time (h)	Yield (%)
1	1a	2a	3a	1.45	86	1.45	90
2	1a	2b	3b	0.45	93	0.5	95
3	1a	2c	3c	1	88	1	94
4	1a	2d	3d	3	71	2.45	78
5	1b	2a	3e	6	78	5	80
6	1b	2b	3f	5	83	4.5	85
7	1b	2c	3g	2	77	1.45	79
8	1c	2a	3h	2.5	81	2	85
9	1c	2d	3i	5	68	4.5	70
10		2a		5	65	5	75
11		2a		6	68	5.5	72
12	1a, 1b	2a	3l	2.5	88	2	90
13	1a, 1c	2a	3m	2.5	85	2	88
14	1a, 1d	2a	3n	3	86	2.45	90
15	1b, 1c	2a	3o	2	90	1.45	92
16	1b, 1d	2a	3p	3	80	2.5	83
17	1a, 1b	2b	3q	2.45	89	2.5	94
18	1a, 1d	2b	3r	3.45	84	3.5	92

Table 4. Synthesis of various TIMs under the catalytic activity of ZnO NRs.

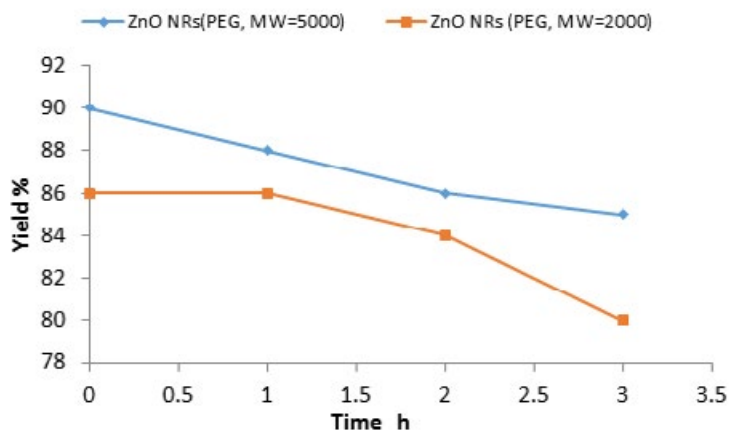


1a: $R_1 = R_2 = R_3 = H$
1b: $R_1 = R_3 = H, R_2 = Cl$
1c: $R_1 = Cl, R_2 = R_3 = H$
1d: $R_1 = R_2 = H, R_3 = Br$

Entry	Indole	TIM	ZnO NRs (2000)		ZnO NRs (5000)	
			Time (h)	Yield (%)	Time (h)	Yield (%)
1	1a	5a	1	96	0.45	96
2	1b	5b	1.5	95	1.25	96
3	1c	5c	2	90	1.45	93
4	1b	5d	2.5	87	2.5	91



Scheme 1. The proposed mechanism for ZnO NRs catalytic activity.

Fig. 5. Recycling and reusability of ZnO NRs in **3a** preparation.

Continuously ZnO NRs (2000) catalyzed different TIMs' synthesis successfully (Table 4, entries 1-4). In the subsequent stage, in order to comprise the ZnO NR (5000) efficacy with its 2000 analog, all the mentioned reactions have been accomplished alternatively. Surprisingly, applying

the same reaction conditions, ZnO NRs 5000 displayed better results in time and yield (Tables 3 and 4). These observations can be due to the major surface area of ZnO NRs 5000 than 2000.

Kong *et al.* reported that ZnO NR has Lewis acid sites (Zn^{2+}) and Lewis basic sites (O^{2-}) [59].

As shown in Scheme 1, initially, a Lewis basic moiety on ZnO NRs reacts with indole and the Lewis acid sites (Zn^{2+}) activate the carbonyl group of isatin and also the oxygen moiety of triethylorthoformate, so the formation of the products is occurred. So, based on this explanation, the larger surface area of ZnO NR (5000) relative to its 2000 analog could be the proof of its more efficient catalytic activity.

Since the recycling and reusability of heterogeneous catalysts, is one of the important items in practical application, the recycling tests of ZnO NRs 2000 & 5000 have been investigated in product **3a** synthesis. The recycled catalyst, subjected to another catalytic reaction under the same reaction conditions. As shown in Fig. 5, the reused catalyst displayed consistent reactivity within 4 runs.

CONCLUSION

ZnO nano-rods were fabricated through a chemical deposition method. Two different capping agents, PEG 2000 & PEG 5000, were applied via this technique. Morphology and nano-structure of obtained crystals were studied with SEM images and XRD patterns. The Wurtzite structure of nano-crystals was confirmed for both capping agents. The results show the one dimensional growth of ZnO nano-rods. PEG can control the shape of nano-crystals. Chemical deposition method was improved with substituting PEG 2000 by PEG 5000 for the first time in this research. The vertically arrays of ZnO NRs were obtained using PEG 2000, but the bow shape of ZnO nanorods were prepared by PEG 5000. The prepared ZnO NRs 2000 & 5000 act as good catalysts for multicomponent condensation of indoles and isatins to form symmetrical and unsymmetrical oxindole derivatives and also triethylorthoformate and indoles to gain their correspondence TIMs. From all catalytic reactions, the nano catalyst recovered by simple filtration and was reused for further condensations without activity loss.

ACKNOWLEDGEMENT

The authors thank the Alzahra University for their financial support.

CONFLICT OF INTEREST

The authors declare that there is no conflict of interests regarding the publication of this manuscript.

REFERENCES

- Gondal MA, Drmosh QA, Yamani ZH, Saleh TA. Synthesis of ZnO nanoparticles by laser ablation in liquid and their annealing transformation into ZnO nanoparticles. *Applied Surface Science*. 2009;256(1):298-304.
- Dong W-G, Kim G-H, Choi J-Y, Yoon J-R, Kim Y-H. A study of the curing behavior of polyamic acid coated on a Cu or Zn layer. *Colloids and Surfaces A: Physicochemical and Engineering Aspects*. 2008;324(1-3):122-5.
- Lewicka ZA, Yu WW, Oliva BL, Contreras EQ, Colvin VL. Photochemical behavior of nanoscale TiO₂ and ZnO sunscreen ingredients. *Journal of Photochemistry and Photobiology A: Chemistry*. 2013;263:24-33.
- Rajeswari R, Prabu HG. Synthesis Characterization, Antimicrobial, Antioxidant, and Cytotoxic Activities of ZnO Nanorods on Reduced Graphene Oxide. *Journal of Inorganic and Organometallic Polymers and Materials*. 2017;28(3):679-93.
- Han N, Wu X, Chai L, Liu H, Chen Y. Counterintuitive sensing mechanism of ZnO nanoparticle based gas sensors. *Sensors and Actuators B: Chemical*. 2010;150(1):230-8.
- Ghosh A, Sharma R, Ghule A, Taur VS, Joshi RA, Desale DJ, et al. Low temperature LPG sensing properties of wet chemically grown zinc oxide nanoparticle thin film. *Sensors and Actuators B: Chemical*. 2010;146(1):69-74.
- Cao J, Wu B, Chen R, Wu Y, Hui Y, Mao B-W, et al. Efficient, Hysteresis-Free, and Stable Perovskite Solar Cells with ZnO as Electron-Transport Layer: Effect of Surface Passivation. *Advanced Materials*. 2018;30(11):1705596.
- Huang J, Wu Y, Gu C, Zhai M, Yu K, Yang M, et al. Large-scale synthesis of flowerlike ZnO nanostructure by a simple chemical solution route and its gas-sensing property. *Sensors and Actuators B: Chemical*. 2010;146(1):206-12.
- Zhang L, Yin L, Wang C, Lun N, Qi Y. Sol-Gel Growth of Hexagonal Faceted ZnO Prism Quantum Dots with Polar Surfaces for Enhanced Photocatalytic Activity. *ACS Applied Materials & Interfaces*. 2010;2(6):1769-73.
- Umar A, Suh EK, Hahn YB. Non-catalytic growth of high aspect-ratio ZnO nanowires by thermal evaporation. *Solid State Communications*. 2006;139(9):447-51.
- Khassin AA, Pelipenko VV, Minyukova TP, Zaikovskii VI, Kochubey DI, Yurieva TM. Planar defect of the nanostructured zinc oxide as the site for stabilization of the copper active species in Cu/ZnO catalysts. *Catalysis Today*. 2006;112(1-4):143-7.
- Tao R-H, Wu J-M, Xiao J-Z, Zhao Y-P, Dong W-W, Fang X-D. Conformal growth of ZnO on TiO₂ nanowire array for enhanced photocatalytic activity. *Applied Surface Science*. 2013;279:324-8.
- He C, Sasaki T, Shimizu Y, Koshizaki N. Synthesis of ZnO nanoparticles using nanosecond pulsed laser ablation in aqueous media and their self-assembly towards spindle-like ZnO aggregates. *Applied Surface Science*. 2008;254(7):2196-202.
- Deng J, Zheng Y-z, Hou Q, Chen J-F, Zhou W, Tao X. Solid-state dye-sensitized hierarchically structured ZnO solar cells. *Electrochimica Acta*. 2011;56(11):4176-80.
- Lin H-F, Liao S-C, Hung S-W. The dc thermal plasma synthesis of ZnO nanoparticles for visible-light photocatalyst. *Journal of Photochemistry and Photobiology A: Chemistry*. 2005;174(1):82-7.
- Zhang L, Ding Y, Povey M, York D. ZnO nanofluids – A

- potential antibacterial agent. *Progress in Natural Science*. 2008;18(8):939-44.
17. Wang X, Summers CJ, Wang ZL. Large-Scale Hexagonal-Patterned Growth of Aligned ZnO Nanorods for Nanophotonics and Nanosensor Arrays. *Nano Letters*. 2004;4(3):423-6.
 18. Chen KJ, Fang TH, Hung FY, Ji LW, Chang SJ, Young SJ, et al. The crystallization and physical properties of Al-doped ZnO nanoparticles. *Applied Surface Science*. 2008;254(18):5791-5.
 19. Vostrikov AA, Fedyeva ON, Shishkin AV, Sokol MY. ZnO nanoparticles formation by reactions of bulk Zn with H₂O and CO₂ at sub- and supercritical conditions: II. Morphology and properties of nanoparticles. *The Journal of Supercritical Fluids*. 2009;48(2):161-6.
 20. Hu J, Odom TW, Lieber CM. Chemistry and Physics in One Dimension: Synthesis and Properties of Nanowires and Nanotubes. *Accounts of Chemical Research*. 1999;32(5):435-45.
 21. Öztürk S, Kılınc N, Taştaltın N, Öztürk ZZ. Fabrication of ZnO nanowires and nanorods. *Physica E: Low-dimensional Systems and Nanostructures*. 2012;44(6):1062-5.
 22. Chen Y, Zhu CL, Xiao G. Reduced-temperature ethanol sensing characteristics of flower-like ZnO nanorods synthesized by a sonochemical method. *Nanotechnology*. 2006;17(18):4537-41.
 23. Choojun S, Hongsith N, Mangkorntong P, Mangkorntong N. Zinc oxide nanobelts by RF sputtering for ethanol sensor. *Physica E: Low-dimensional Systems and Nanostructures*. 2007;39(1):53-6.
 24. Chang CC, Chang CS. Site-specific growth to control ZnO nanorods density and related field emission properties. *Solid State Communications*. 2005;135(11-12):765-8.
 25. Atrak K, Ramazani A, Taghavi Fardood S. A novel sol-gel synthesis and characterization of MgFe₂O₄@ γ -Al₂O₃ magnetic nanoparticles using tragacanth gel and its application as a magnetically separable photocatalyst for degradation of organic dyes under visible light. *Journal of Materials Science: Materials in Electronics*. 2018;29(8):6702-10.
 26. Atrak K, Ramazani A, Taghavi Fardood S. Green synthesis of amorphous and gamma aluminum oxide nanoparticles by tragacanth gel and comparison of their photocatalytic activity for the degradation of organic dyes. *Journal of Materials Science: Materials in Electronics*. 2018;29(10):8347-53.
 27. Taghavi Fardood S, Ramazani A, Golfar Z, Joo SW. Green synthesis of Ni-Cu-Zn ferrite nanoparticles using tragacanth gum and their use as an efficient catalyst for the synthesis of polyhydroquinoline derivatives. *Applied Organometallic Chemistry*. 2017;31(12):e3823.
 28. Moradi S, Taghavi Fardood S, Ramazani A. Green synthesis and characterization of magnetic NiFe₂O₄@ZnO nanocomposite and its application for photocatalytic degradation of organic dyes. *Journal of Materials Science: Materials in Electronics*. 2018;29(16):14151-60.
 29. Sorbiun M, Shayegan Mehr E, Ramazani A, Taghavi Fardood S. Biosynthesis of Ag, ZnO and bimetallic Ag/ZnO alloy nanoparticles by aqueous extract of oak fruit hull (Jaft) and investigation of photocatalytic activity of ZnO and bimetallic Ag/ZnO for degradation of basic violet 3 dye. *Journal of Materials Science: Materials in Electronics*. 2017;29(4):2806-14.
 30. Fardood ST, Ramazani A, Moradi S. A Novel Green Synthesis of Nickel Oxide Nanoparticles Using Arabic Gum. *Chemistry Journal of Moldova*. 2017;12(1):115-8.
 31. Sorbiun M, Shayegan Mehr E, Ramazani A, Taghavi Fardood S. Green Synthesis of Zinc Oxide and Copper Oxide Nanoparticles Using Aqueous Extract of Oak Fruit Hull (Jaft) and Comparing Their Photocatalytic Degradation of Basic Violet 3. *International Journal of Environmental Research*. 2018;12(1):29-37.
 32. Fardood ST, Ramazani A, Joo SW. Eco-friendly synthesis of magnesium oxide nanoparticles using arabic Gum. *J Appl Chem Res*. 2018; 12(1): 8-15.
 33. Taghavi Fardood S, Ramazani A, Moradi S, Azimzadeh Asiabi P. Green synthesis of zinc oxide nanoparticles using arabic gum and photocatalytic degradation of direct blue 129 dye under visible light. *Journal of Materials Science: Materials in Electronics*. 2017;28(18):13596-601.
 34. Fardood ST, Golfar Z, Ramazani A. Novel sol-gel synthesis and characterization of superparamagnetic magnesium ferrite nanoparticles using tragacanth gum as a magnetically separable photocatalyst for degradation of reactive blue 21 dye and kinetic study. *Journal of Materials Science: Materials in Electronics*. 2017;28(22):17002-8.
 35. Shayegan Mehr E, Sorbiun M, Ramazani A, Taghavi Fardood S. Plant-mediated synthesis of zinc oxide and copper oxide nanoparticles by using ferulago angulata (schlecht) boiss extract and comparison of their photocatalytic degradation of Rhodamine B (RhB) under visible light irradiation. *Journal of Materials Science: Materials in Electronics*. 2017;29(2):1333-40.
 36. Fardood ST, Ramazani A, Joo SW. Sol-gel Synthesis and Characterization of Zinc Oxide Nanoparticles Using Black Tea Extract. *Journal of Applied Chemical Research*. 2017; 11(4): 8-17.
 37. Khrenov V, Klapper M, Koch M, Müllen K. Surface Functionalized ZnO Particles Designed for the Use in Transparent Nanocomposites. *Macromolecular Chemistry and Physics*. 2005;206(1):95-101.
 38. Jiaqiang X, Yuping C, Daoyong C, Jianian S. Hydrothermal synthesis and gas sensing characters of ZnO nanorods. *Sensors and Actuators B: Chemical*. 2006;113(1):526-31.
 39. Bhuiyan MRA, Rahman MK. Synthesis and Characterization of Ni Doped ZnO Nanoparticles. *International Journal of Engineering and Manufacturing*. 2014;4(1):10-7.
 40. Izaki M, Omi T. Transparent zinc oxide films prepared by electrochemical reaction. *Applied Physics Letters*. 1996;68(17):2439-40.
 41. Iwata K, Tampo H, Yamada A, Fons P, Matsubara K, Sakurai K, et al. Growth of ZnO and device applications. *Applied Surface Science*. 2005;244(1-4):504-10.
 42. Liang C, Sasaki T, Shimizu Y, Koshizaki N. Pulsed-laser ablation of Mg in liquids: surfactant-directing nanoparticle assembly for magnesium hydroxide nanostructures. *Chemical Physics Letters*. 2004;389(1-3):58-63.
 43. Singh AK, Viswanath V, Janu VC. Synthesis, effect of capping agents, structural, optical and photoluminescence properties of ZnO nanoparticles. *Journal of Luminescence*. 2009;129(8):874-8.
 44. Ramazani A, Dabbaghi A, Gouranlou F. Synthesis of Amphiphilic Co-network through Click Chemistry Reactions: A Review. *Current Organic Chemistry*. 2018;22(4):362-9.
 45. Hosseinzadeh Z, Ramazani A, Hosseinzadeh K, Razzaghi-

- Asl N, Gouranlou F. An Overview on Chemistry and Biological Importance of Pyrrolidinone. *Current Organic Synthesis*. 2018;15(2):166-78.
46. Nikoofar K, Khademi Z. Barbituric Acids in Organic Transformations, An Outlook to the Reaction Media. *Mini-Reviews in Organic Chemistry*. 2017;14(2):143-73.
 47. Hosseini-Sarvari M, Tavakolian M. Preparation, characterization, and catalysis application of nanorods zinc oxide in the synthesis of 3-indolyl-3-hydroxy oxindoles in water. *Applied Catalysis A: General*. 2012;441-442:65-71.
 48. Das D, Nath BC, Phukon P, kalita A, Dolui SK. Synthesis of ZnO nanoparticles and evaluation of antioxidant and cytotoxic activity. *Colloids and Surfaces B: Biointerfaces*. 2013;111:556-60.
 49. Mbule PS, Kim TH, Kim BS, Swart HC, Ntwaeaborwa OM. Effects of particle morphology of ZnO buffer layer on the performance of organic solar cell devices. *Solar Energy Materials and Solar Cells*. 2013;112:6-12.
 50. Rai P, Jo J-N, Lee I-H, Yu Y-T. Fabrication of flower-like ZnO microstructures from ZnO nanorods and their photoluminescence properties. *Materials Chemistry and Physics*. 2010;124(1):406-12.
 51. Khorsand Zak A, Abd. Majid WH, Abrishami ME, Yousefi R. X-ray analysis of ZnO nanoparticles by Williamson-Hall and size-strain plot methods. *Solid State Sciences*. 2011;13(1):251-6.
 52. Prabhu YT, Rao KV, Kumar VSS, Kumari BS. X-Ray Analysis by Williamson-Hall and Size-Strain Plot Methods of ZnO Nanoparticles with Fuel Variation. *World Journal of Nano Science and Engineering*. 2014;04(01):21-8.
 53. Agasti N, Kaushik NK. One Pot Synthesis of Crystalline Silver Nanoparticles. *American Journal of Nanomaterials*. 2014; 2(1): 4-7.
 54. Sundberg R. *The Chemistry of Indoles* (Academic. New York: Academic Press; 1996.
 55. Subba Reddy BV, Rajeswari N, Sarangapani M, Prashanthi Y, Ganji RJ, Addlagatta A. Iodine-catalyzed condensation of isatin with indoles: A facile synthesis of di(indolyl)indolin-2-ones and evaluation of their cytotoxicity. *Bioorganic & Medicinal Chemistry Letters*. 2012;22(7):2460-3.
 56. Mohammadi Ziarani G, Moradi R, Badieli A, Lashgari N, Moradi B, Abolhasani Soorki A. Efficient green synthesis of 3,3-di(indolyl)indolin-2-ones using sulfonic acid functionalized nanoporous SBA-Pr-SO₃H and study of their antimicrobial properties. *Journal of Taibah University for Science*. 2015;9(4):555-63.
 57. Verma M, Tripathi M, Saxena AK, Shanker K. Antiinflammatory activity of novel indole derivatives. *European Journal of Medicinal Chemistry*. 1994;29(12):941-6.
 58. Garbe TR, Kobayashi M, Shimizu N, Takesue N, Ozawa M, Yukawa H. Indolyl Carboxylic Acids by Condensation of Indoles with α -Keto Acids. *Journal of Natural Products*. 2000;63(5):596-8.
 59. Kong XY, Wang ZL. Spontaneous Polarization-Induced Nanohelices, Nanosprings, and Nanorings of Piezoelectric Nanobelts. *Nano Letters*. 2003;3(12):1625-31.